Eur Biophys J (1997) 26: 433–445 

ARTICLE

**Roman Meyer · Stefan H. Heinemann**

# Temperature and pressure dependence of *Shaker* $K^+$ channel N- and C-type inactivation

Received: 17 May 1997 / Accepted: 18 July 1997

**Abstract** *Shaker* B potassium channels undergo rapid N-type and slow C-type inactivation. While N-type inactivation is supposed to be mediated by occlusion of the pore by the N-terminal protein structure, the molecular mechanisms leading to C-type inactivation are less well understood. Considering N-type inactivation as a model for a protein conformational transition, we investigated inactivation of heterologously expressed *Shaker* B potassium channels and mutants thereof, showing various degrees of C-type inactivation, under high hydrostatic (oil) pressure. In addition to the derived apparent activation and reaction volumes ($\Delta V$), experiments at various temperatures yielded estimates for enthalpic ($\Delta H$) and entropic ($T\Delta S$) contributions. N-type inactivation was accelerated by increasing temperature and slowed by high hydrostatic pressure yielding at equilibrium $\Delta H = 76$ kJ/mole, $T\Delta S = 82$ kJ/mole, and $\Delta V = 0.18$ nm$^3$ indicating that the transition to the N-type inactivated state is accompanied by an increase in volume and a decrease in order. N-terminally deleted *Sh*Δ6–46 constructs with additional mutations at either position 449 or 463 were used to investigate C-type inactivation. In particular at high temperatures, inactivation occurred in two phases indicating more than one process. At equilibrium the following values were estimated for the major inactivation component of mutant *Sh*Δ6–46 T449A: $\Delta H = -64$ kJ/mole, $T\Delta S = -60$ kJ/mole, and $\Delta V = -0.25$ nm$^3$, indicating that the C-type inactivated state occupies a smaller volume and is more ordered than the noninactivated state. Thus, hydrostatic pressure affects N- and C-type inactivation in opposite ways.

**Key words** Potassium channel · Inactivation · Hydrostatic pressure · Thermodynamics · Site-directed mutagenesis

R. Meyer · S. H. Heinemann (✉)
Max-Planck-Gesellschaft z.F.d.W. e.V.,
AG Molekulare und zelluläre Biophysik,
Drackendorfer Strasse 1, D-07747 Jena, Germany,
(e-mail: ite@rz.uni-jena.de)

## Introduction

Voltage-gated potassium channels ($K^+$ channels) undergo at least two types of inactivation (Hoshi et al. 1991). N-type inactivation is thought to occur through a so-called "ball-and-chain" mechanism which was initially proposed for the inactivation of sodium channels (Armstrong and Bezanilla 1977). The N-terminal end of the $K^+$ channel subunit presumably forms an inactivating domain which can obstruct the ion channel pore from the cytoplasmic side and thereby cause an interruption of the ion flow, i.e. it leads to inactivation (Hoshi et al. 1990). Even after deletion of the N-terminal structure, a much slower inactivating component remains in *Shaker* B channels. Since a C-terminal *Shaker* splice variant (*Shaker* A) shows a much faster inactivation of this kind (Hoshi et al. 1991) it was termed C-type inactivation. Several recent studies, however, have shown that amino-acid residues in the pore region and the permeating ions play an important role in this inactivation (López-Barneo et al. 1993; DeBiasi et al. 1993; Schlief et al. 1996). Therefore, the term P-type inactivation would actually be more appropriate.

While a compelling body of evidence was compiled for the mechanism of N-type inactivation, not very much is known about the molecular mechanism of C-type inactivation. What can be concluded at the moment is that, during C-type inactivation, structural rearrangements at the external entry of the pore must be occurring as the accessibility of amino-acid residues in the outer pore region to chemically modifying agents shows a clear dependence on the inactivation state (Liu et al. 1996; Schlief et al. 1996).

Therefore, at least two distinct molecular mechanisms are leading to inactivation in $K^+$ channels: During N-type inactivation the presumably very flexible N-terminal ball structure must diffuse – tethered with a peptide chain to the rest of the channel protein – to its "receptor" where it binds via hydrophobic forces (Hoshi et al. 1990; Murrell-Lagnado and Aldrich 1993). It should be noted that this reaction is very much facilitated in the open channel state which results in a strong coupling of inactivation and ac-

tivation. C-type inactivation, on the other hand, is associated with a conformational change of the external pore entry whose nature is not known. These two types of inactivation can be distinguished by their sensitivities to endopeptidases and the pore blocker tetraethylammonium (TEA). N-type inactivation is sensitive to application of cytosolic endopeptidases (Hoshi et al. 1990) and shows a competition with intracellular TEA; extracellular TEA, on the other hand, competes with C-type inactivation (Grissmer and Cahalan 1989; Choi et al. 1991). However, at least the latter criterion is not unambiguous and a coupling of N- and C-type inactivation even complicates the situation (Baukrowitz and Yellen 1995).

The motivation of the following study was to gain more insight into the molecular mechanisms underlying these intra-protein conformational changes by investigating their thermodynamic properties in two types of experiments. Activation enthalpy and entropy were measured by changing the temperature in the range of about 10–30 °C. Information about the volume changes accompanying the protein conformational transitions, i.e. the apparent activation volumes, was obtained by measuring the inactivation kinetics at hydrostatic pressure of up to 50 MPa (≈ 500 atmospheres).

All experiments were carried out with *Shaker* B $K^+$ channels and mutants thereof expressed in *Xenopus* oocytes. *Shaker* B served as an example for an N-type inactivating channel; C-type inactivation was investigated in mutants of *Shaker* B Δ6–46 channels, i.e. *Shaker* B with a partially deleted N-terminal structure. In the following this construct will be referred to as *Sh*Δ. In order to increase the speed of C-type inactivation, various pore mutations were introduced in the background *Sh*Δ at positions T449 and A463 (Hoshi et al. 1991; López-Barneo et al. 1993; Schlief et al. 1996).

Preliminary results of this work have been presented in abstract form (Meyer and Heinemann 1995).

## Materials and methods

### Oocyte preparation and mRNA injection

Stage V oocytes were obtained from *Xenopus laevis*, anaesthetized with 0.2% tricaine in ice water, according to standard methods (Stühmer et al. 1992). The follicular layer was removed by collagenase treatment prior to mRNA injection. About 50 nl mRNA in a concentration ranging from 0.05 to 0.5 μg/ ml was injected into the oocytes. Electrophysiological recordings were started after 12 h of incubation at 17 °C.

The following $K^+$ channel clones were used: *Shaker* B, and mutants of *Sh*Δ: T449A, T449K, T449Q, T449S, A463V (Hoshi et al. 1991; López-Barneo et al. 1993; Schlief et al. 1996). The template DNA was linearized with *Sst*I and capped cRNA was synthesized with the T7 mMessage mMachine Kit (Ambion, Austin, TX, USA).

### Electrophysiological recordings

For experiments at different temperatures the two-electrode voltage clamp as well as the patch-clamp technique were used. The temperature was controlled by a Peltier element underneath the bath chamber and was regulated with a temperature control unit. The temperature in solution was measured with a thermo-element. Experiments were performed in the temperature range of approximately 10 to 30 °C. Whole-cell currents were measured with a two-electrode voltage clamp amplifier (Turbo TEC 10CD, npi electronic, Tamm, Germany). Intracellular electrodes were filled with 2 M KCl and had a resistance between 0.5 and 1.0 MΩ. An EPC-9 electronic amplifier (HEKA elektronik, Lambrecht, Germany) was used for patch-clamp experiments. Data acquisition was performed with the Pulse + PulseFit software package (HEKA elektronik) running on Macintosh Computers (Apple Computer Inc., Cupertino, CA, USA). Data analysis was performed with the programs PulseFit (HEKA elektronik) and IgorPro (WaveMetrics Inc., Lake Oswego, OR, USA). Data values are given as mean ± s.e.m.

The following external solutions were used (in mM): K10Na107: 10 KCl, 107 NaCl, 10 Hepes, 1.8 $CaCl_2$; NFR: 115 NaCl, 2.5 KCl, 1.8 $CaCl_2$, 10 Hepes; K50Na67: 50 KCl, 67.5 NaCl, 1.8 $CaCl_2$, 10 Hepes; K-Ringer: 115 KCl, 1.8 $CaCl_2$, 10 Hepes. In most cases the temperature dependence of inactivation was tested in K10Na107. For experiments at different pressures solutions containing 2.5 mM $K^+$ and 115 mM $K^+$ were also used. The internal solution for patch-clamp experiments was K-EGTA: 115 KCl, 1.8 EGTA, and 10 Hepes. All solutions were titrated to pH 7.2.

### High pressure apparatus

Patch-clamp experiments at various pressures were performed with a pressure apparatus similar to that described by Heinemann et al. (1987b). After obtaining an excised patch, a glass cup, which was connected to the patch pipette holder, was placed in front of the pipette tip such that the pipette tip dipped into this cup. Together with this small bath solution reservoir, the patch was then moved out of the main bath chamber; subsequently it was placed into the pressure vessel filled with pure paraffin oil. The pressure vessel was sealed with a lid of stainless steel which contained the necessary high-pressure electrical feedthroughs for the patch electrode, the ground electrode and the thermistor. Pressure was applied by pressing oil with a hand-driven pump into the pressure vessel. Data records were taken about 5 minutes after changing pressure in order to reach a temperature equilibrium. Temperature was measured by a thermistor which was placed inside the vessel; it was controlled with a Haake K15 thermostat (Haake, Mess-Technik GmbH, Karlsruhe, Germany) which was connected to a water-filled jacket around the pressure vessel.

In addition to this high-pressure patch-clamp configuration, in some cases a miniaturized two-electrode voltage-

clamp unit which fits into the pressure vessel of 20 mm width and 60 mm height (Schmalwasser and Heinemann, in preparation) was used for recording currents from entire oocytes under high pressure.

### Data analysis

Inactivation time constants, $\tau_i$, were determined from exponential fits to the decline of the current. The inverse time constants were used as rate constants, $k_i$. Recovery from inactivation at –100 mV was measured in double-pulse experiments with increasing interpulse duration as shown in the inset of Fig. 1B.

The temperature dependencies of the rate constants were analyzed according to Arrhenius:

$$\ln k = \ln A - \frac{E_a}{RT} \tag{1}$$

where $R$ indicates the gas constant, $T$ the absolute temperature, and $ln\ A$ is a preexponential factor. From the slope of an Arrhenius plot ($ln\ k$ versus $1/T$) the activation energy ($E_a$) is obtained. According to the transition-state theory, the free enthalpy for the activation step ($\Delta G^{\ddagger}$) is related to the rate constant by:

$$k = \kappa \frac{k_B T}{h} \cdot e^{(-\Delta G^{\ddagger}/RT)} \tag{2}$$

where $k_B$ is Boltzmann's constant, and $h$ Planck's constant. The transmission coefficient $\kappa$ was assumed to be unity. The activation free enthalpy consists of an enthalpic ($\Delta H^{\ddagger}$) and an entropic part ($\Delta S^{\ddagger}$): $\Delta G^{\ddagger} = \Delta H^{\ddagger} - T\Delta S^{\ddagger}$. From Arrhenius plots both quantities can be obtained by assuming that the rate constants were measured under constant pressure and constant membrane potential.

$$\Delta H^{\ddagger} = E_a - RT \tag{3}$$

$$\Delta S^{\ddagger} = R\left(\ln A - \ln\left(\frac{k_B T}{h}\right)\right) \tag{4}$$

In the range of –20 to +50 mV there was, indeed, only a very small voltage dependence of N- and C-type inactivation which was neglegted for the calculation of $\Delta H^{\ddagger}$ and $T\Delta S^{\ddagger}$. For the recovery from N-type and C-type inactivation a small voltage dependence of the rate constant was observed in the range of –120 to –70 mV. In these cases the voltage dependent term was not determined explicitly; instead it was included in the activation enthalpy which then slightly depended on the membrane potential. $\Delta G^{\ddagger}$, $\Delta H^{\ddagger}$, and $T\Delta S^{\ddagger}$ were calculated for 293 K (20 °C).

Thermodynamic equilibrium data were estimated from inactivation time constants and the relative steady-state current ($h_{inf}$ = steady-state current/peak current) at the end of the test pulse. Rate constants for inactivation ($k_i$) and recovery ($k_r$) at +50 mV were evaluated according to:

$$k_r = \frac{h_{inf}}{\tau_i} \tag{5}$$

$$k_i = \frac{1 - h_{inf}}{\tau_i} \tag{6}$$

The resulting equilibrium constant, $K = k_i/k_r$, was plotted versus the inverse temperature (Van't Hoff plots). Enthalpy ($\Delta H$), entropy ($\Delta S$), and free enthalpy ($\Delta G$) changes were obtained from a linear fit to:

$$\ln K = -\frac{\Delta H}{RT} + \frac{\Delta S}{R} \tag{7}$$

From the pressure (P) dependence of the rate constants an apparent activation volume ($\Delta V^{\ddagger}$) can be estimated according to:

$$\left(\frac{\partial \ln k}{\partial P}\right)_T = -\frac{\Delta V^{\ddagger}}{RT} \tag{8}$$

The logarithm of the rate constant was plotted versus pressure and fitted to a linear equation (Fig. 5C). From the slope an activation volume was evaluated according to Eq. (8).

Macro-patches under high hydrostatic pressure are not very stable and the recording time had to be minimized. Therefore, in some cases rate constants for the recovery from inactivation were only estimated from one double-pulse experiment with a fixed interpulse duration and assuming a single-exponential time course.

## Results

### Temperature dependence of N-type inactivation

N-type inactivation was studied with wild-type *Shaker* B channels. In Fig. 1A current traces from *Shaker* B at different temperatures are shown. As N-type inactivation was much faster than C-type inactivation, for analysis of the onset of inactivation only the initial, fast decline of current was used. Inactivation was clearly accelerated by increasing temperature (Fig. 1A). The recovery rate was determined from double-pulse experiments (Fig. 1B). A single exponential time course for recovery was observed indicating that the channels were mainly N-type inactivated during the first test pulse. Recovery from inactivation at –100 mV revealed a weaker temperature dependence than that of inactivation. This resulted in a lower activation energy for recovery than for inactivation (Fig. 1C). Free activation enthalpy ($\Delta G^{\ddagger}$), activation enthalpy ($\Delta H^{\ddagger}$), and activation entropy ($\Delta S^{\ddagger}$) were estimated and are summarized in Table 1. For inactivation the determined activation enthalpy ($\Delta H^{\ddagger}$) was greater than the free activation enthalpy ($\Delta G^{\ddagger}$). This resulted in a positive activation entropy ($\Delta S^{\ddagger}$), while for the recovery a negative activation entropy was determined.

### Temperature dependence of C-type inactivation of *Sh*ΔT449A

In Fig. 2A current traces of *Sh*Δ T449A at different temperatures are shown. At low temperatures the decline of

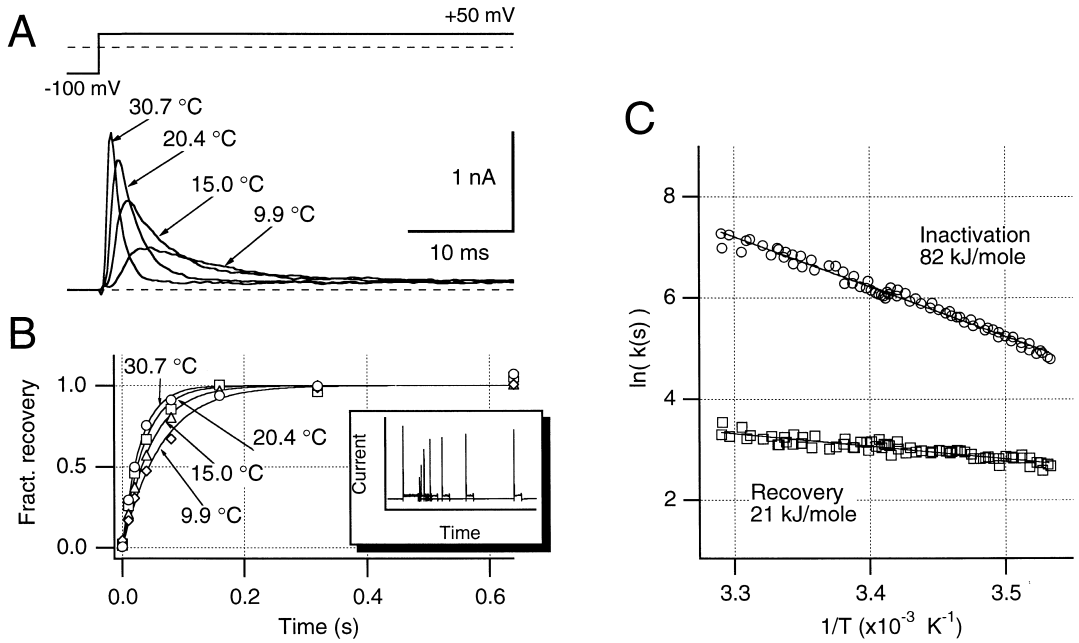


**Fig. 1A–C** Temperature dependence of N-type inactivation. The data were recorded from on-cell patches with K10Na107 in the pipette and K-EGTA in the bath. The holding potential was –100 mV and the channels were activated by voltage steps to +50 mV. **A** Current traces of *Shaker* B channels recorded at the indicated temperatures. **B** Recovery from N-type inactivation at the indicated temperatures. The fraction of recovery was determined according to ([a2–a0]/[a1–a0]). a1 and a2 indicate the peak currents of first and second pulse and a0 the steady-state current at the end of the first pulse. The continuous curves indicate results of single-exponential data fits. *Inset*: Example for a double-pulse experiment with increasing duration between the pulses. This protocol was employed to measure the recovery from the inactivated state at –100 mV. **C** Arrhenius plots for the rate of N-type inactivation (at +50 mV) and the rate of recovery from N-type inactivation (at –100 mV) based on one experiment. Activation energies resulting from the linear fits (see Eq. (1)) are indicated. All displayed data points are from one experiment

the current seemed to be single-exponential, but a more detailed analysis revealed that the inactivation which remains after removal of N-type inactivation has two components. The proportion of the slow component increased with increasing temperature and was observable under our experimental conditions down to about 18 °C. The traces were fitted with a double exponential equation and both resulting time constants were used for analysis. The corresponding Arrhenius plots are shown in Fig. 2C. For the main (fast) component an activation energy of about 65 kJ/mole was estimated which is similar to that found for N-type inactivation of *Shaker* B (~75 kJ/mole, see Table 1). The slow component revealed a much higher activation energy (~165 k/mole).

Temperature dependence of recovery was determined from double pulse experiments at –100 mV. Again, two components could be distinguished. The main part recovered slowly, while only a smaller part recovered more rapidly (Fig. 2B). The fraction of fast recovery increased with increasing temperature. To show the double exponential time course of recovery more clearly, data were also plotted on a logarithmic time base in Fig. 2B. For both recovery components relatively high activation energies were determined (Fig. 2C, Table 1).

## Estimation of ΔG, ΔH and TΔS at equilibrium

As inactivation and recovery were determined at different potentials, the evaluated rate constants cannot be used for the calculation of an equilibrium constant without information about the voltage dependence of the rates. Although the voltage dependence of recovery and inactivation were small at hyperpolarized or depolarized potentials, alterations of the rate constants during activation, i.e. at intermediate potentials, cannot be excluded. To determine not only activation quantities but also thermodynamic quantities valid for equilibrium, recovery rates at +50 mV were estimated for *Shaker* B and *Sh*ΔT449A. For N-type inactivation of *Shaker* B the amplitude of the slowly C-type inactivating current component was taken as the steady-state level. For *Sh*ΔT449A the amplitude of the slowly inactivating current component was taken to be the steady-state level of the fast current component. It was assumed that an equilibrium between inactivation and recovery was reached. The steady-state current was estimated from a single-exponential fit to the initial decline of the current. Recovery rates at +50 mV were determined according to Eq. (5). Current traces and analysis plots for *Shaker* B and *Sh*ΔT449A are shown in Fig. 3. The estimated recovery rates and activation energies for recovery at +50 mV were for both channel types comparable to those determined at –100 mV (Fig. 3B and 3E).

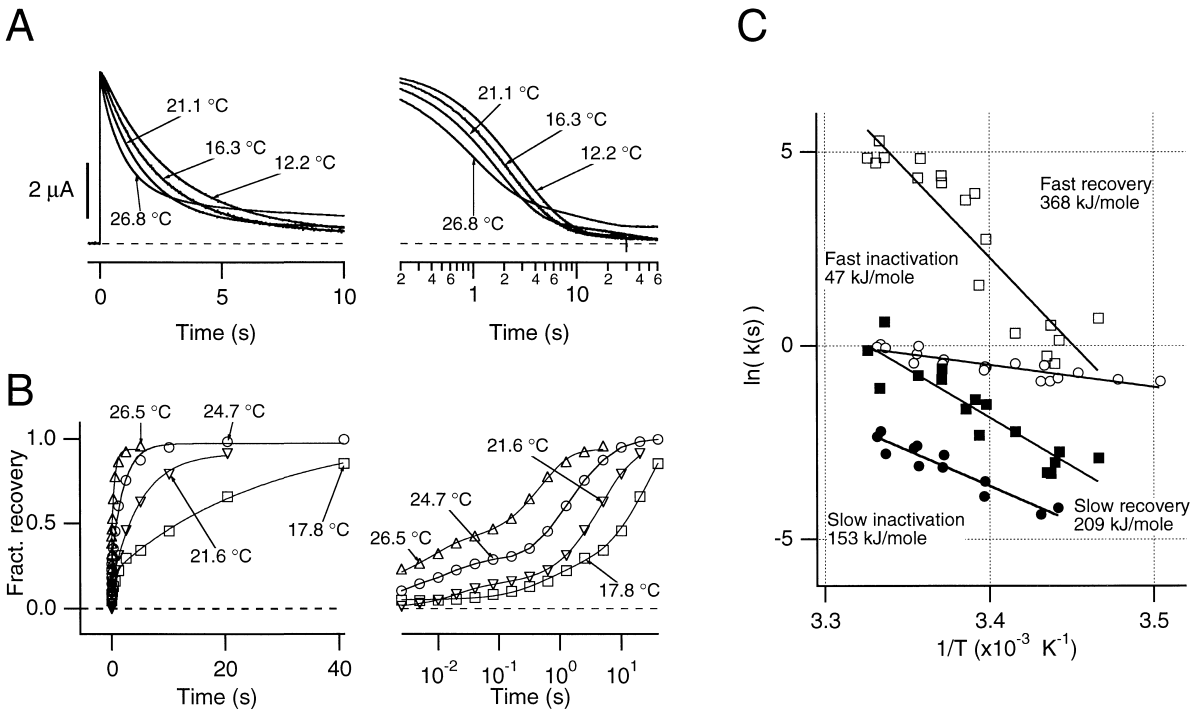


**Fig. 2A–C** Temperature dependence of C-type inactivation of mutant *Sh*ΔT449A. **A** Current traces recorded at the indicated temperatures with the two-electrode voltage-clamp technique with solution K10Na107 in the bath. Traces were scaled to maximal current. Inactivation was best described by a double-exponential equation. To enhance visibility of the two phases of inactivation, the data are shown in the right panel on a logarithmic time base. Both components of inactivation were speeded up with temperature; the relative proportion of the slower component increased with temperature. **B** Recovery of *Sh*ΔT449A from inactivation was measured in double-pulse experiments with increasing interpulse duration. The time course of recovery revealed two phases which can be clearly seen by plotting the data on a logarithmic time base (right panel). The fraction of the fast recovery component increased with increasing temperature. **C** Arrhenius plots for both components of the inactivation (at +50 mV) and the recovery (–100 mV). The data were fit with straight lines (Eq. (1)) and the resulting activation energies are indicated in the figure

**Table 1** Thermodynamic activation quantities determined from experiments at different temperatures. Values are given as mean ± s.e.m. The number of experiments is given in parentheses. The time constants were extrapolated from the Arrhenius fits to 20°C

| Channel type (*n*) | $\tau$ (s) | $\Delta G^{\ddagger}$ (kJ/mole) | $\Delta H^{\ddagger}$ (kJ/mole) | $T\Delta S^{\ddagger}$ (kJ/mole) |
|---|---|---|---|---|
| | Inactivation (at +50 mV) | | | |
| *Shaker* B (5) | 0.0029 ± 0.0002 | 57.4 ± 0.2 | 75 ± 4 | 18 ± 4 |
| *Sh*ΔT449A (fast) (6) | 2.66 ± 0.36 | 74.0 ± 0.3 | 66 ± 6 | –8 ± 6 |
| *Sh*ΔT449A (slow) (3) | 38.0 ± 9.2 | 80.4 ± 0.6 | 167 ± 4 | 86 ± 3 |
| *Sh*ΔT449K (6) | 0.100 ± 0.038 | 65.7 ± 0.7 | 40 ± 4 | –26 ± 5 |
| *Sh*ΔT449Q (5) | 0.097 ± 0.022 | 65.8 ± 0.5 | 54 ± 8 | –11 ± 8 |
| *Sh*ΔT449S (fast) (4) | 0.0062 ± 0.0014 | 59.1 ± 0.6 | 77 ± 12 | 18 ± 12 |
| *Sh*ΔT449S (slow) (4) | 0.066 ± 0.017 | 64.8 ± 0.7 | 56 ± 8 | –9 ± 8 |
| *Sh*ΔA463V (3) | 0.094 ± 0.010 | 65.9 ± 0.3 | 60 ± 4 | –6 ± 4 |
| | Recovery from inactivation (at –100 mV) | | | |
| *Shaker* B (4) | 0.046 ± 0.005 | 64.2 ± 0.3 | 31 ± 7 | –33 ± 7 |
| *Sh*ΔT449A (fast) (3) | 0.203 ± 0.043 | 67.7 ± 0.5 | 384 ± 34 | 316 ± 34 |
| *Sh*ΔT449A (slow) (6) | 8.33 ± 0.85 | 76.8 ± 0.3 | 188 ± 23 | 112 ± 23 |
| *Sh*ΔT449K (6) | 4.07 ± 0.77 | 74.9 ± 0.4 | 128 ± 12 | 53 ± 13 |
| *Sh*ΔT449Q (6) | 4.34 ± 0.72 | 75.1 ± 0.4 | 137 ± 7 | 62 ± 8 |
| *Sh*ΔT449S (5) | 22.6 ± 5.0 | 79.1 ± 0.5 | 120 ± 6 | 41 ± 7 |
| *Sh*ΔA463V (3) | 1.81 ± 0.16 | 73.1 ± 0.2 | 157 ± 11 | 84 ± 11 |

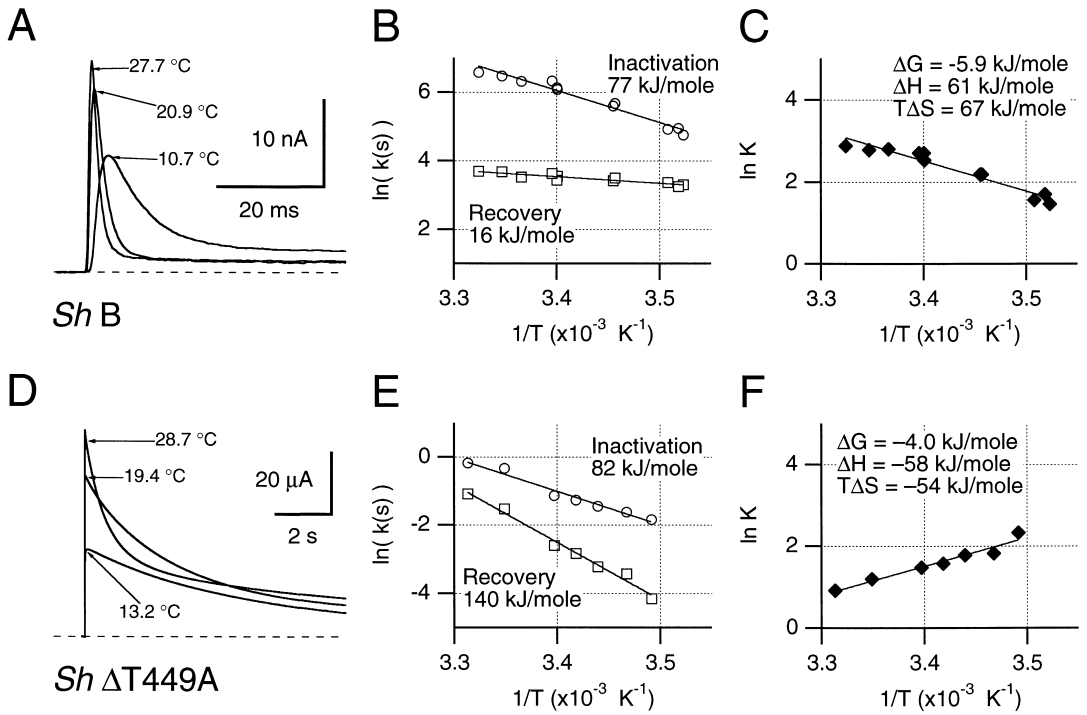


**Fig. 3A–F** Estimation of equilibrium thermodynamic parameters. **A** Current traces of *Shaker* B recorded at the indicated temperatures at +50 mV in the on-cell patch-clamp configuration. **B** Arrhenius plots for N-type inactivation and recovery from N-type inactivation of *Shaker* B. Rate constants were determined according to Eqs. 5 and 6. Steady-state current was obtained at the end of the pulse and was normalized to the peak current. Resulting activation energies are indicated. **C** Van't Hoff plots for N-type inactivation at +50 mV. The equilibrium constants were calculated from the rate constants: $K = k_i / k_r$; ΔG, ΔH, and TΔS were determined according to Eq. (7). **D** Current traces recorded from *Sh*ΔT449A at the indicated temperatures with the two-electrode voltage-clamp technique. Traces were fitted to a single-exponential function. Rate constants of inactivation and recovery were obtained according to Eqs. (5) and (6). **E** Arrhenius plots for C-type inactivation of *Sh*ΔT449A; analysis similar to **B**. **F** Van't Hoff plots for C-type inactivation at +50 mV; analysis similar to **C**

Equilibrium constants for N-type inactivation of *Shaker* B and for the fast component of C-type inactivation of *Sh*ΔT449A were determined from the rate constants for inactivation and recovery at +50 mV. From van't Hoff plots the changes in free enthalpy (ΔG), enthalpy (ΔH) and entropy (ΔS) were estimated (Fig. 3C and 3F). For *Shaker* B enthalpy and entropy were positive; the negative ΔG results from a greater entropic part. N-type inactivation of *Shaker* B is, therefore, favored by the entropy. For C-type inactivation investigated with *Sh*ΔT449A negative enthalpy and entropy values were obtained; the negative ΔG results from a greater enthalpic contribution indicating that C-type inactivation is primarily driven by enthalpic energies.

## Temperature dependence of C-type inactivating channel mutants

As C-type inactivation of *Sh*Δ and *Sh*ΔT449A is rather slow, channel mutants with faster C-type inactivation were used. These mutants carry a single amino-acid exchange at either position 449 or 463 (*Sh*ΔT449K, *Sh*ΔT449Q, *Sh*ΔT449S, *Sh*ΔA463V) in the background of *Sh*Δ. For the mutants *Sh*ΔT449K (Fig. 4A), *Sh*ΔT449Q (Fig. 4B), and *Sh*ΔA463V (Fig. 4D) inactivation time courses could be approximated with single-exponential functions. This, however, does not exclude the possibility that these mutants also have a slow inactivation component like *Sh*ΔT449A. The second component may not have been visible because of insufficient pulse lengths (≤1 s). Activation energies in the range of 40–60 kJ/mole were determined for C-type inactivation of these mutants; for recovery at –100 mV much greater activation energies were obtained (Fig. 4A, 4B, and 4D; Table 1). $\Delta G^{\ddagger}$, $\Delta H^{\ddagger}$, $T\Delta S^{\ddagger}$ values for these mutants were estimated and are summarized in Table 1. Activation enthalpies are nearly equal to activation energies; small negative $\Delta S^{\ddagger}$ values were evaluated for inactivation and positive $\Delta S^{\ddagger}$ values for recovery (Table 1). This agrees with the results found for the fast inactivation and slow recovery components of *Sh*ΔT449A channels.

The inactivation of *Sh*ΔT449S clearly showed a double-exponential time course. Therefore, the current traces were fitted according to a double-exponential equation and both resulting rate constants were used for analysis (Fig. 4C, Table 1). The thermodynamic parameters of the slow component were comparable to those of the other mutants with enhanced C-type inactivation. In contrast, for

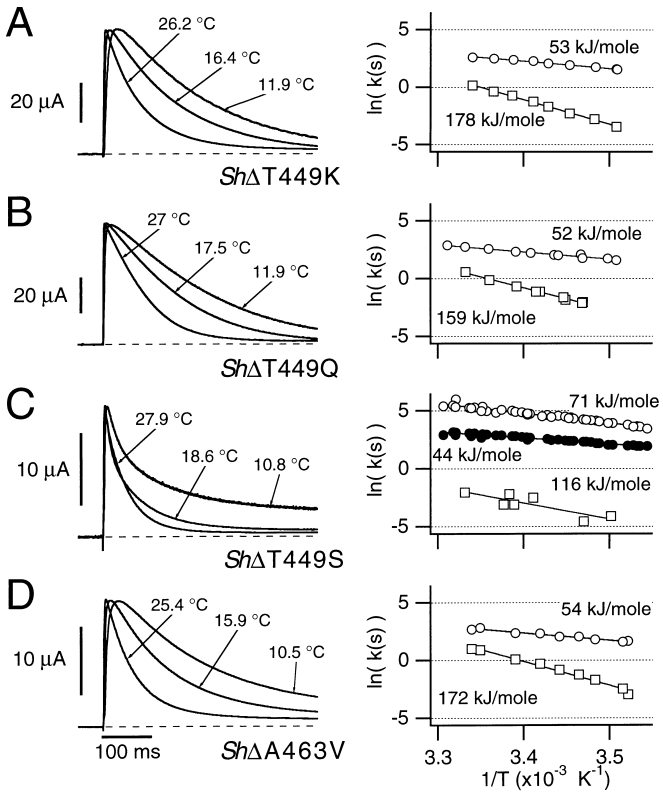


**Fig. 4A–D** Temperature dependence of various *Sh*Δ mutants. Data were recorded with the two-electrode voltage-clamp technique with the solution K10Na107 in the bath. *Left panels:* Current traces recorded from (**A**) *Sh*ΔT449K, (**B**) *Sh*ΔT449Q, (**C**) *Sh*ΔT449S, and (**D**) *Sh*ΔA463V at the indicated temperatures. *Right panels:* Arrhenius plots for inactivation (+50 mV, open circles) and recovery from inactivation (–100 mV, open squares). In **A**, **B**, and **D** the time constants for the C-type inactivation were determined from single-exponential fits to the declining phase of the traces. For *Sh*ΔT449S (**C**) the declining phase was fitted to a double-exponential function. Both resulting rate constants were used for determination of the indicated activation energies (fast component: open circles; slow component: filled circles). Recovery from inactivation of this mutant was measured in inside-out patches with K-EGTA in the bath and K10Na107 in the pipette; it could be described by a single-exponential time course

the fast component the values for $\Delta G^{\ddagger}$, $\Delta H^{\ddagger}$, and $T\Delta S^{\ddagger}$ were similar to those found for N-type inactivation of *Shaker* B (Table 1). The recovery from inactivation at –100 mV revealed a single-exponential time course. Qualitatively, the activation energy and activation entropy were similar to those found for the other C-type inactivating *Sh*Δ mutants (Fig. 4C, Table 1).

## Pressure dependence of N-type inactivation

Information about volume changes accompanying the molecular rearrangements during inactivation were obtained by performing patch-clamp and two-electrode voltage-clamp experiments at different hydrostatic (oil) pressures.

**Table 2** Apparent activation volumes ($\Delta V^{\ddagger}$) determined from experiments at various hydrostatic pressures. Values are given as mean ± s.e.m. The number of experiments is given in parentheses

| Channel type | $\Delta V^{\ddagger}$ ($nm^3$) | $\Delta V^{\ddagger}$ ($nm^3$) |
|---|---|---|
| | Inactivation (at +50 mV) | Recovery (at –100 or –80 mV) |
| *Shaker* B | 0.105 ± 0.008 (6) | –0.073 ± 0.010 (4) |
| *Sh*ΔT449A | –0.125 ± 0.009 (8) | 0.108 ± 0.022 (4) |
| *Sh*ΔT449K | –0.064 ± 0.017 (3) | n.d. |
| *Sh*ΔT449Q | –0.064 ± 0.017 (2) | n.d. |
| *Sh*ΔT449S (slow) | –0.058 ± 0.009 (2) | n.d. |
| *Sh*ΔT449S (fast) | 0.054 ± 0.008 (2) | n.d. |
| *Sh*ΔA463V | 0.022 ± 0.040 (3) | n.d. |

In Fig. 5A current traces recorded from *Shaker* B channels in a membrane patch under various pressures are shown. N-type inactivation as well as activation of these channels was slowed with increasing pressure. Assuming that the channels inactivate after activation and that activation is faster than inactivation, the influence of activation on the inactivation time course should be small in the late phase of the current decline. Therefore, this late current decline was used for analysis. The logarithm of the determined inactivation rate constants was plotted as a function of pressure yielding a linear relationship (Fig. 5C). From the slope of a linear fit to the data, positive apparent activation volumes ($\Delta V^{\ddagger}$) were determined (Fig. 5C, Table 2).

Recovery from N-type inactivation (at –100 mV) was accelerated with increasing pressure, indicating a negative activation volume (Fig. 5B, C, Table 2). As inactivation (+50 mV) and recovery (–100 mV) were investigated at different potentials, the evaluated data cannot simply be used to calculate an apparent reaction volume (ΔV). Therefore, the recovery rate at +50 mV was measured from the steady-state current according to Eq. 5 in order to estimate the influence of the potential on the recovery rate. Comparisons of recovery rates determined at +50 mV and –100 mV from identical two-electrode voltage-clamp experiments revealed that the recovery was slower at +50 mV than at –100 mV. However, the estimated apparent activation volumes were nearly identical. In patch-clamp experiments the steady-state current was relatively small and, therefore, the estimated recovery rates had a rather big statistical error: $\Delta V^{\ddagger} = -0.022 \pm 0.022\ nm^3$ ($n = 6$). A positive apparent reaction volume of about $+0.15\ nm^3$ was estimated from the pressure dependencies of inactivation and recovery rates at +50 mV according to Eqs. 5 and 6. From the difference of activation volumes for inactivation at +50 mV and recovery at –100 mV an apparent reaction volume of $0.18\ nm^3$ was obtained (Table 3).

## Pressure dependence of C-type inactivation

Current traces recorded from *Sh*ΔT449A channels in the inside-out patch-clamp configuration at various hydro-

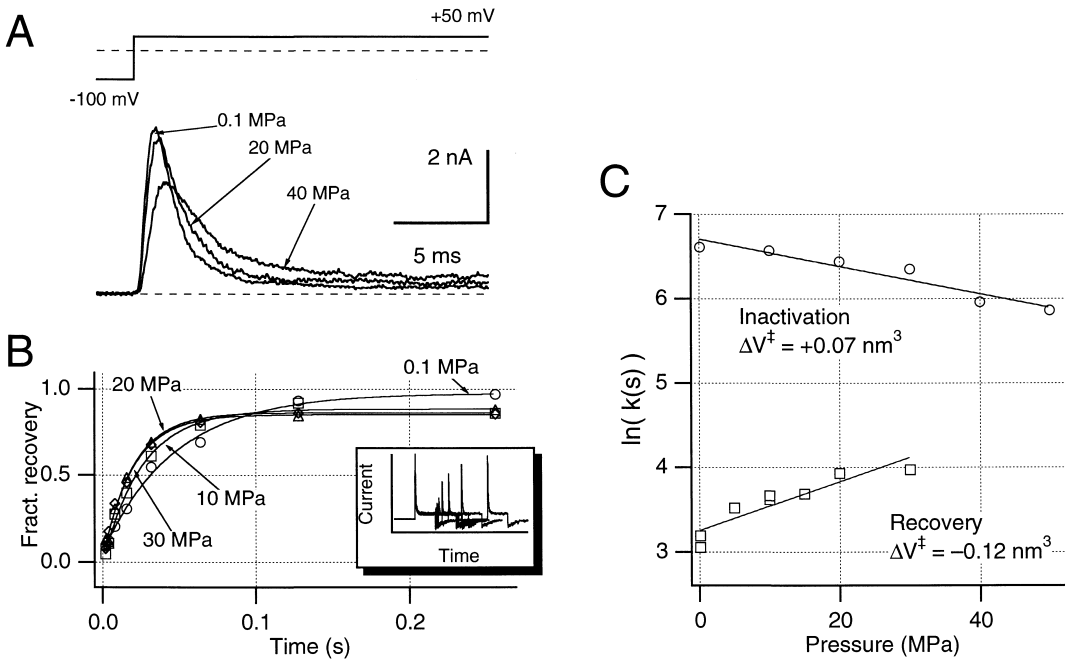


**Fig. 5A–C** Pressure dependence of N-type inactivation. **A** Current traces recorded from *Shaker* B channels at the indicated hydrostatic pressures. The data were obtained from inside-out patches with NFR in the pipette and K-EGTA in the bath. The holding potential was –80 mV and the channels were activated by voltage steps to +50 mV. **B** Recovery from N-type inactivation (–80 mV) at the indicated pressures. The data were obtained from outside-out patches with K50Na67 in the pipette and K-EGTA in the bath. *Inset:* Example for a double-pulse experiment with increasing duration at –80 mV between the pulses. **C** Logarithm of the rate constants for N-type inactivation and recovery as a function of pressure. The indicated apparent activation volumes ($\Delta V^{\ddagger}$) were estimated according to Eq. (8)

static pressures are shown in Fig. 6A. In excised patches inactivation of *Sh*ΔT449A was considerably faster than in two-electrode voltage-clamp experiments. Furthermore, as pressure experiments were performed at room temperature, no prominent slow component of inactivation could be measured. Thus, we only studied the pressure dependence of the main fast inactivation component. As shown in Fig. 6A, increasing pressure *accelerated* C-type inactivation of *Sh*ΔT449A. Owing to the limited life time of macro patches under high pressure, the rate of recovery from inactivation could only be estimated by applying two consecutive pulses, separated by a constant duration at –100 mV (8 s). From the ratio of the peak currents of the second and first pulse, recovery rates were estimated by assuming a single-exponential function. Analysis of inactivation and recovery is shown in Fig. 6B. For C-type inactivation a negative apparent activation volume was obtained; for recovery from C-type inactivation $\Delta V^{\ddagger}$ was positive. These thermodynamic parameters are qualitatively the opposite of those found for the process of N-type inactivation of *Shaker* B channels.

As C-type inactivation was nearly complete during depolarizations of excised patches, it was not possible to measure accurately a recovery rate from the steady-state current at +50 mV. However, as estimated from two-electrode voltage-clamp experiments, the recovery rates at –100 mV and +50 mV are similar. Assuming that this is also true for excised patches, an apparent reaction volume can be estimated from the apparent activation volumes for inactivation at +50 mV and recovery at –100 mV. This resulted in a negative apparent reaction volume of about –0.25 $nm^3$ (Table 3). Similarly to the comparison of the reaction entropy, the sign of the apparent reaction volume of

**Table 3** Equilibrium thermodynamic parameters determined at +50 mV. *K*, Δ*G*, Δ*H*, and *T*Δ*S* were calculated for 293 K. Values are given as mean ± s.e.m. The number of experiments is given in parentheses. The reaction volume (Δ*V*) for *Shaker* B was obtained from experiments performed at 22 °C, 26 °C, and 29 °C, whereas *Sh*ΔT449A was investigated at 21 °C and 25 °C. ΔV values were determined from rate constants of inactivation at +50 mV and recovery at –100 mV, both determined in identical patches

| Channel type | *K* | Δ*G* (kJ/mole) | Δ*H* (kJ/mole) | *T*Δ*S* (kJ/mole) | Δ*V* ($nm^3$) |
|---|---|---|---|---|---|
| *Shaker* B | 12.9 ± 1.0 (3) | –6.2 ± 0.2 (3) | 76 ± 8 (3) | 82 ± 8 (3) | 0.18 ± 0.03 (4) |
| *Sh*ΔT449A | 6.8 ± 2.3 (3) | –4.4 ± 0.8 (3) | –64 ± 17 (3) | –60 ± 16 (3) | –0.25 ± 0.02 (4) |

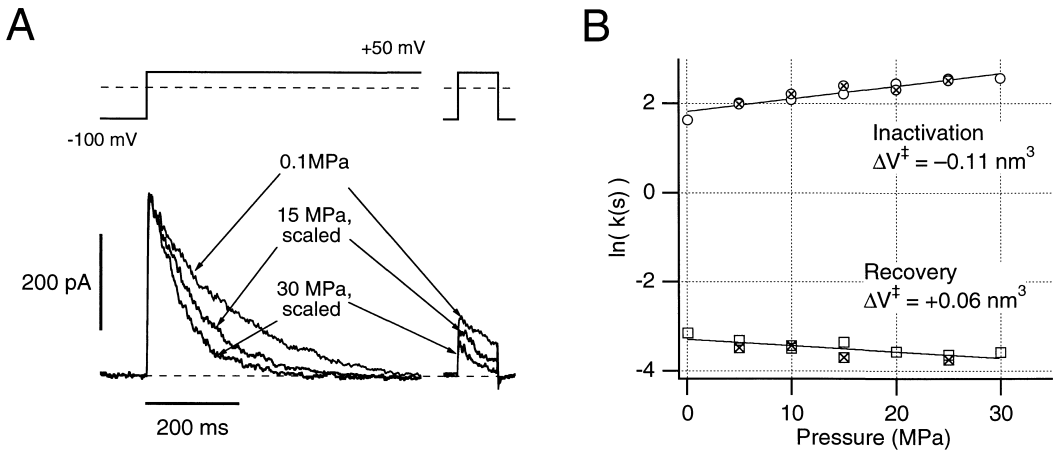


**Fig. 6 A, B** Pressure dependence of C-type inactivation of *Sh*ΔT449A. **A** Current traces recorded from double-pulse experiments with *Sh*ΔT449A at the indicated pressures. The data were obtained from inside-out patches with NFR in the pipette and K-EGTA in the bath. In order to visualize the difference in time constant, the traces were scaled to the maximal current. The second pulse, given after an 8-s interval at –80 mV, was used for the estimation of the recovery rate. **B** Logarithm of the rate constants for C-type inactivation and recovery as a function of pressure. The indicated apparent activation volumes ($\Delta V^{\ddagger}$) were estimated according to Eq. (8). Symbols with a cross in the center denote data points obtained while the pressure was decreased, indicating the reversibility of the observed effects

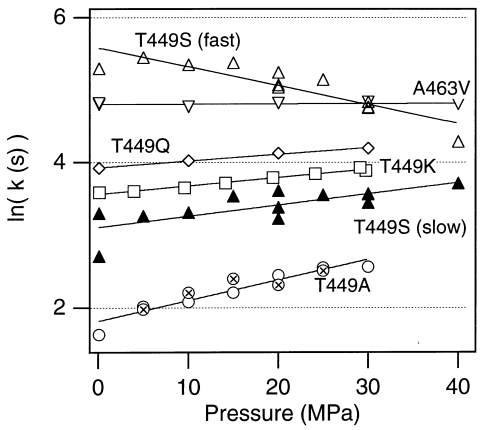


**Fig. 7** Pressure dependence of the C-type inactivation of *Sh*Δ mutants. The logarithm of the rate constants determined from the indicated *Sh*Δ mutants was plotted as a function of pressure. Apparent activation volumes were estimated from linear fits according to Eq. (8) (mean values are listed in Table 1). For the mutants *Sh*ΔT449A, *Sh*ΔT449K, and *Sh*ΔT449Q negative activation volumes were determined. The fast and slow component of *Sh*ΔT449S were analyzed separately

N-type inactivation is the opposite of that obtained for C-type inactivation.

Experiments at different pressures were also performed with other *Shaker* B mutants (*Sh*ΔT449K, *Sh*ΔT449Q, *Sh*ΔT449S, *Sh*ΔA463V) which show various rates of C-type inactivation. C-type inactivation of *Sh*ΔT449K and *Sh*ΔT449Q was accelerated by increasing pressure (Fig. 7). The resulting apparent activation volumes were negative, but smaller than those found for *Sh*ΔT449A. As known from experiments at different temperatures, *Sh*ΔT449S showed a double-exponential inactivation. The fast component of inactivation was slowed, while the slow component was accelerated by pressure (Fig. 7). The estimated apparent activation volumes had, therefore, opposite signs. For *Sh*ΔA463V time constants of inactivation were only marginally altered by pressure (Fig. 7). Mean values of the apparent activation volumes are summarized in Table 2.

## Discussion

In this study we investigated the thermodynamic properties of $K^+$ channel inactivation by measuring the dependence of inactivation phenomena on temperature and hydrostatic pressure. We used *Shaker* B channels and mutants thereof in order to characterize N- and C-type inactivation. N-type inactivation, whose temperature dependence was already intensively studied, was considered as a process which served as a control owing to the relatively simple underlying molecular mechanism. C-type inactivation, which is much more complex in terms of molecular mechanisms, proved to display thermodynamic properties reflecting this complexity.

### N-type inactivation

Investigation of the temperature dependence of N-type inactivation of *Shaker* B revealed a high activation enthalpy, while the activation enthalpy for recovery from inactivation was low (Table 1). These results confirm data by Nobile et al. (1997). Studies of the interaction of *Shaker* B N-terminal peptides with channels also yielded a high temperature dependence for binding of peptides and a very low temperature dependence for release of peptides (Murrell-Lagnado and Aldrich 1993). The thermodynamic

parameters determined for peptide-mediated inactivation revealed the same tendency as our data (binding of peptides: $\Delta G^{\ddagger} = 36$ kJ/mole; $\Delta H^{\ddagger} = 110$ kJ/mole; $T\Delta S^{\ddagger} = 74$ kJ/mole; release of peptides: $\Delta G^{\ddagger} = 65$ kJ/mole; $\Delta H^{\ddagger} = -0.3$ kJ/mole; $T\Delta S^{\ddagger} = -65$ kJ/mole).

Equilibrium constants for N-type inactivation of *Shaker* B were determined from inactivation and recovery rates, estimated at +50 mV. From van't Hoff plots the free enthalpy, enthalpy, and entropy for N-type inactivation were evaluated (Table 3). The negative free enthalpy of N-type inactivation is a product of overcompensating the positive enthalpy by the entropic term. Murrell-Lagnado and Aldrich (1993) estimated equilibrium constants for peptide binding and release at +50 mV ($\Delta G = -34$ kJ/mole; $\Delta H = 111$ kJ/mole; $\Delta S = 145$ kJ/mole). Changes in enthalpy as well as in entropy were positive and the negative $\Delta G$ resulted from the greater entropic component. This agrees with our results (Table 3).

Hoshi et al. (1990) showed that positively charged as well as hydrophobic amino acids in the N-terminus are important for N-type inactivation. Murrell-Lagnado and Aldrich (1993) suppose that the charged amino acids enhance diffusion and increase the effective concentration of N-terminal "balls" near the pore. The binding, on the other hand, should be mainly stabilized by hydrophobic interactions. The thermodynamic characteristics of such hydrophobic interactions were investigated by transfer experiments. Transfer of nonpolar molecules from a nonpolar liquid phase to an aqueous solution is accompanied by a decrease of the entropy (Creighton 1993). This is generally explained by a reordering of water molecules surrounding the nonpolar molecules. During the generation of hydrophobic interactions, the number of water molecules neighbouring hydrophobic residues decreases and the entropy increases. The effect of hydrophobic binding should be most prominent during the unbinding process (recovery) as no preceding diffusion is involved. In accordance with a hydrophobic binding model, $T\Delta S^{\ddagger}$ of N-type recovery is negative and $\Delta H^{\ddagger}$ is small, (Table 1). Furthermore, the free enthalpy at equilibrium is dominated by the positive entropic term (Table 3). This can also be taken as an indication for the important influence of hydrophobic interaction on N-type inactivation. However, positively charged amino acids are also necessary for fast N-type inactivation (Hoshi et al. 1990) and a dominating enthalpic term was determined for this process (Table 1). The obtained activation enthalpy of inactivation may, therefore, result from both, diffusion and ionic or polar interactions of the N-terminus with the pore region.

Although macro-patches from *Xenopus* oocytes were not very stable under high hydrostatic pressure, the method of pressurizing patch-clamp holders in an oil-filled pressure vessel (Heinemann et al. 1987b) proved useful for determining volume changes associated with conformational transitions of cloned wild-type and mutated ion channel proteins. From the pressure dependence of N-type inactivation positive activation volumes were determined (Table 2). Thus, on the way from the open to the inactivated state, the volume occupied by the channel and the system environment, i.e. the surrounding solution and the membrane, transiently increases. Similarly to these results, the inactivation of sodium channels is also slowed by high pressure as reported by Conti et al. (1982a) and Heinemann et al. (1987a). This similarity presumably reflects related molecular mechanisms for inactivation according to a "ball and chain" model which was originally proposed for the inactivation of sodium channels (Armstrong and Bezanilla 1977).

Recovery from N-type inactivation at –100 mV is associated with a negative activation volume (Fig. 5C). From estimated recovery rates at +50 mV negative activation volumes with similar values were determined. These data were used to estimate a positive reaction volume of about 0.15 $nm^3$, indicating that the difference between the total volumes of an N-type inactivated and a noninactivated *Shaker* channel including its energetically coupled environment is equivalent to the volume change associated with the transition of about 50 water molecules from liquid to ice structure (Conti 1986). However, as volume changes accompanied with hydrophobic interactions are still discussed controversially (Lüdemann 1988), the observed volume increase cannot be taken as unambiguous indicator for hydrophobic binding of the N-terminus to the pore.

The energy associated with a volume change is part of the enthalpy ($\Delta H = \Delta U + P\Delta V$). At atmospheric pressure (~ 0.1 MPa) this energetic contribution ($P\Delta V$) is very small (≈ 6 J/mole). Therefore, the influence of the volume change on the enthalpy at atmospheric pressure could be neglected. Interestingly, the positive activation volume of N-type inactivation is paralleled by a positive activation entropy and the negative activation volume of recovery by a negative activation entropy (Tables 1 and 2). In a simple consideration, it can be speculated that the greater volume of the N-type inactivated state induces a decrease of order and, therefore, an increase of entropy.

## Osmotic versus hydrostatic pressure

Changes in unilateral osmotic pressure were also reported to affect ion channel kinetics. A slowing of both, N-type inactivation and recovery from N-type inactivation of *Shaker* B channels, could be induced by increasing the osmolarity of the intracellular solution in inside-out patches (Starkus et al. 1995). Hyperosmolar internal solutions, therefore, increase the energy barrier between the open and inactivated states, while no effect of high external osmolarity on N-type inactivation was observed (Starkus et al. 1995). As shown in this study, hydrostatic pressure also slowed N-type inactivation, but recovery from N-type inactivation was accelerated. Hydrostatic pressure seems not only to influence the energy barrier but also the energy difference between open and inactivated state. Therefore, kinetic effects of N-type inactivation induced by hydrostatic and osmotic pressure cannot be compared in a simple way. Hydrostatic pressure influences the internal interactions of the protein as well as the interactions with the environment, i.e. membrane and water. Osmotic pressure, on the

other hand, mainly changes the availability of water molecules for specific interactions with the protein surface, thus, both methods provide complementary approaches for studying the thermodynamics of protein conformational changes.

## Inactivation of *Sh*Δ mutants has two components

Attempting to study the thermodynamics of C-type inactivation we realized that the inactivation remaining after N-terminal deletions (Δ6–46) of *Shaker* B channels consists of more than a single component. As shown in Fig. 2, in particular at high temperature, the slowly inactivating mutant *Sh*ΔT449A clearly revealed two components for inactivation and for recovery from inactivation at room temperature. The fast fraction is the major component of inactivation and it has properties which are indicative of a C-type mechanism. Fast inactivation was slowed by high $[K^+]_0$ which is typical for C-type inactivation (López-Barneo et al. 1993). The slow recovery of *Sh*ΔT449A was also accelerated by elevated $[K^+]_0$, a phenomenon also reported for recovery from C-type inactivation of Kv1.4 channels (Rasmusson et al. 1995). The slow recovery constituted the main fraction and, therefore, reflected the recovery from the rapidly C-type inactivated state. The component of fast recovery was not affected by $[K^+]_o$ (data not shown).

The proportion of the slow inactivation as well as that of the fast recovery increased with temperature (Fig. 2A, B), which corroborates the indication that the slow inactivation and the fast recovery belong to the same process. Presently it is not clear if these components reflect a novel type of inactivation or whether they are just a modulated form of C-type inactivation. The latter possibility is supported by the strong variability of the magnitude of these components and, in particular, by the observed alterations upon excision of membrane patches. Furthermore, although N-type inactivation was largely removed by the N-terminal deletion (Δ6–46), it is feasible that a residual, very slow N-type inactivation remained. The determined activation energy for the slow inactivation was higher than that determined for C-type inactivation. Also the estimated activation entropy was positive and not negative as evaluated for C-type inactivation of the other *Sh*Δ mutants. But this negative correlation is certainly not a sufficient criterion for excluding a C-type mechanism for the slow inactivation. In terms of thermodynamic parameters the second component is more similar to N-type inactivation. The rate constant determined for the fast recovery is in the range of N-type recovery. However, N-type inactivation of *Shaker* B was accompanied by a small activation energy, whereas for the fast recovery of *Sh*ΔT449A a very high activation energy was observed. Considering that the substantial deletion in the N-terminus would significantly change the absolute magnitude of temperature dependence, it is still possible that, in particular at high temperatures, a truncated N-terminal structure could contribute to inactivation.

During long depolarizing pulses (60 s) also for the mutant *Sh*ΔT449Q a second slow inactivation could be observed (not shown). However, as most of the *Sh*Δ mutants inactivate much more rapidly than the wild type or *Sh*ΔT449A, the slow inactivation was not always detectable.

The rapidly inactivating mutant *Sh*ΔT449S also showed a double exponential time course for inactivation. In contrast to the results obtained from mutant *Sh*ΔT449A, both inactivation components were very fast. The faster component revealed a temperature as well as pressure dependence which was similar to that of N-type inactivation of *Shaker* B channels. The results obtained for the slow component were comparable to those of the major C-type inactivation component of the other mutants. Recovery from inactivation was dominated by a single exponential time course indicating that both types of inactivation can occur in parallel. Thus far, the molecular mechanism of the rapid phase of *Sh*ΔT449S inactivation remains elusive.

## Temperature dependence of the main C-type inactivation component

The mutants *Sh*ΔT449K, *Sh*ΔT449Q, and *Sh*ΔA463V mainly showed a single exponential time course of C-type inactivation. In terms of the thermodynamic characteristics, the fast component of inactivation and the slow one of recovery from *Sh*ΔT449A inactivation and the slowly inactivating component of *Sh*ΔT449S show similar properties compatible with this major C-type mechanism.

In contrast to the N-type inactivation mechanism, the temperature dependence of C-type inactivation is smaller than that determined for recovery from C-type inactivation. In addition, the activation energies of C-type inactivation are smaller than that obtained for N-type inactivation. However, this difference is relatively small and may not be sufficient for distinguishing between N- and C-type inactivation. The temperature dependencies of recovery from N- or C-type inactivation, however, were very different. Only a small activation energy could be detected for N-type recovery, whereas for C-type recovery much higher activation energies were determined (Table 1). Therefore, this difference might be used to discriminate between N- and C-type inactivation in *Shaker* B channels.

For C-type inactivation of the mutant *Sh*ΔT449A similar values for $\Delta H^{\ddagger}$ and $T\Delta S^{\ddagger}$ were obtained as for the faster C-type inactivating mutants (*Sh*ΔT449K, *Sh*ΔT449Q, *Sh*ΔT449S, *Sh*ΔA463V). No clear correlation between the speed of C-type inactivation and $\Delta H^{\ddagger}$ or $T\Delta S^{\ddagger}$ of *Sh*Δ mutants could be determined. The free activation enthalpy of the investigated *Sh*Δ mutants differs by about 10 kJ/mole which is in the range of the determined standard deviations. Therefore, possible differences of $\Delta H^{\ddagger}$ and $T\Delta S^{\ddagger}$ induced by the amino acid exchanges could not be detected.

Lee and Deutsch (1990) as well as Pahapill and Schlichter (1990) investigated the temperature dependence of inactivating $K^+$ currents in human T-lymphocytes. These currents are supposed to be mediated by the $K^+$ channel Kv1.3 which is known to undergo C-type inactivation. Lee and Deutsch reported a lower temperature dependence for

inactivation than for recovery (at –90 mV). This is in accordance with our results determined for C-type inactivation of *Sh*Δ mutants. Furthermore $\Delta G^{\ddagger}$, $\Delta H^{\ddagger}$, and $T\Delta S^{\ddagger}$ for inactivation given by Pahapill and Schlichter ($\Delta G^{\ddagger>} = 67$ kJ/mole, $\Delta H^{\ddagger} = 55$ kJ/mole, and $T\Delta S^{\ddagger} = -12$ kJ/mole) are similar to the values obtained for the *Sh*Δ mutants (Table 1).

For the fast inactivation of *Sh*ΔT449A equilibrium constants were estimated and from van't Hoff plots ΔG, ΔH, and TΔS at +50 mV were determined. Negative enthalpy and entropy values were obtained. The free enthalpy is dominated by a high negative enthalpy. C-type inactivation, which is assumed to be a result of structural changes in the outer mouth of the pore, is, therefore, enthalpic driven indicating that the inactivated state is more ordered than the open state. It is interesting to note that the closed (deactivated) state of *Shaker* B channels is less ordered than the open (activated) state as reported by Rodríguez and Bezanilla (1996). The N-type inactivated state is also less ordered than the open state.

## Pressure dependence of C-type inactivation

C-type inactivation of several *Shaker* B mutants was accelerated with increasing pressure. The activated state seemed to have a smaller volume than the open state. This was consistent for all *Sh*Δ mutants with a single amino-acid exchange at position 449 (Table 2). Only for mutant *Sh*ΔA463V almost no change of inactivation rate was found upon increasing pressure. Pressure dependence of recovery from C-type inactivation was tested with *Sh*ΔT449A yielding a positive activation volume. Assuming that recovery rates reveal only a minor voltage dependence, a negative apparent reaction volume for *Sh*ΔT449A was estimated from the activation volumes evaluated for inactivation at +50 mV and for recovery at –100 mV (Table 3). A smaller volume should force the molecules into a more ordered state which is consistent with the estimated negative entropy for C-type inactivation (Table 3).

The apparent activation volumes of inactivation of *Sh*Δ mutants seem to depend on the speed of inactivation (Fig. 7). With increasing rate constants apparent activation volumes decrease and finally change sign (*Sh*ΔA463V and the fast component of *Sh*ΔT449S). This result for the first time correlates site-directed alterations of channel protein structures and volume changes associated with protein conformational transitions. Lacking an insight into the mechanism involved, it is presently not possible to provide a molecular interpretation.

For the fast inactivation component of *Sh*ΔT449S a positive activation volume was determined which is contrary to the results found for the other C-type inactivating mutants. As N-type inactivation of *Shaker* B is also accompanied by a positive activation volume, it may be speculated that the fast component of *Sh*ΔT449S is possibly mediated by a kind of residual N-type mechanism. However, *Sh*ΔT449A also revealed two kinetically different inactivation components whose thermodynamic parameters are not compatible with N-type inactivation. Therefore, it remains elusive whether or not the fast inactivating component of *Sh*ΔT449S is mediated by a new or a modulated C-type mechanism.

N- and C-type inactivation are known to be mediated by different mechanisms. This is also reflected in a different thermodynamic behavior. Temperature as well as pressure influence the kinetics of N- and C-type inactivation differently. This difference can be used as a complementary tool for distinguishing between both types of inactivation. For *Sh*Δ mutants an additional inactivation component was observed. Inactivation seems, therefore, to be more complex than assumed thus far.

## Pressure dependence of ion channel function

Effects of hydrostatic pressure on biological functions are of particular importance for deep-sea divers. The *High Pressure Nervous Syndrome* (HPNS), occurring during exposure to hyperbaric pressure in the range of 2–20 MPa, is characterized by an increased excitability of the central nervous system. The involvement of ion channels in the HPNS is discussed controversially (for review see Kendig and Grossman 1987). Although transmitter release by exocytosis is more sensitive to pressure than ion channel function (Heinemann et al. 1987a), it is feasible that a reduction of $K^+$ currents can contribute to the hyperexcitability of the nervous system observed under hyperbaric conditions. Conti et al. (1982b) already pointed out that activation of squid-axon $K^+$ channels are slowed down by high pressure; similar results were obtained for *Shaker* B channels (see Fig. 5A). Although N-type inactivation of *Shaker* B channels showed a positive apparent reaction volume, favoring the non-inactivated state, the large negative apparent reaction volume determined for C-type inactivation of mutant *Sh*ΔT449A indicates that, on the average, $K^+$ current can be reduced by high pressure as most $K^+$ channels undergo C-type inactivation to some extent.

**Acknowledgements** We would like to thank A. Roßner, A. Grimm, and H. Schmalwasser for technical assistance and R. W. Aldrich for providing us with *Shaker* B cDNA. This work was supported by the Deutsche Forschungsgemeinschaft "SFB 197, Biological and Model Membranes".

## References

Armstrong CM, Bezanilla F (1977) Inactivation of the sodium channel. II. Gating current experiments. J Gen Physiol 70:567–590

Baukrowitz T, Yellen G (1995) Modulation of $K^+$ current by frequency and external $[K^+]$: A tale of two inactivation mechanisms. Neuron 15:951–960

Choi KL, Aldrich RW, Yellen G (1991) Tetraethylammonium blockade distinguishes two inactivation mechanisms in voltage-activated $K^+$ channels. Proc Natl Acad Sci USA 88:5092–5095

Conti F (1986) The relationship between electrophysiological data and thermodynamics of ion channel conformations. In: Ritchie JM (ed) Ion channel in neural membranes. Liss, New York, pp 25–42

Conti F, Fioravanti R, Segal JR, Stühmer W (1982a) Pressure dependence of the sodium currents of squid giant axon. J Membr Biol 69:23–34

Conti F, Fioravanti R, Segal JR, Stühmer W (1982b) Pressure dependence of the potassium currents of squid giant axon. J Membr Biol 69:35–40

Creighton TE (1993) Proteins: Structures and molecular properties, 2nd edn. Freemann, New York

De Biasi M, Hartmann HA, Drewe JA, Taglialatela M, Brown AM, Kirsch GE (1993) Inactivation determined by a single site in $K^+$ pores. Pflügers Arch 422:354–363

Grissmer S, Cahalan MD (1989) TEA prevents inactivation while blocking open $K^+$ channels in human T-lymphocytes. Biophys J 55:203–206

Heinemann SH, Conti F, Stühmer W, Neher E (1987a) Effects of hydrostatic pressure on membrane processes. Sodium channels, calcium channels, and exocytosis. J Gen Physiol 90:765–778

Heinemann SH, Stühmer W, Conti F (1987b) Single acetylcholine receptor channel currents recorded at high hydrostatic pressures. Proc Natl Acad Sci USA 84:3229–3233

Hoshi T, Zagotta WN, Aldrich RW (1990) Biophysical and molecular mechanisms of *Shaker* potassium channel inactivation. Science 250:533–538

Hoshi T, Zagotta WN, Aldrich RW (1991) Two types of inactivation in *Shaker* $K^+$ channels: Effects of alterations in the carboxy-terminal region. Neuron 7:547–556

Kendig JJ, Grossman Y (1987) How can hyperbaric pressure increase central nervous system excitability? In: Jannasch HW, Marquis RE, Zimmerman AM (eds) Current perspectives of high pressure biology. Academic Press, London, pp159–169

Lee SC, Deutsch C (1990) Temperature dependence of $K^+$-channel properties in human T-lymphocytes. Biophys J 57:49–62

Liu Y, Jurmann ME, Yellen G (1996) Dynamic rearrangement of the outer mouth of a $K^+$ channel during gating. Neuron 16:859–867

López-Barneo J, Hoshi T, Heinemann SH, Aldrich RW (1993) Effects of external cations and mutations in the pore region on C-type inactivation of *Shaker* potassium channels. Rec Chan 1:61–71

Lüdemann HD (1988) Influence of pressure on protein conformation. Makromol Chem Macromol Symp 17:29–38

Meyer R, Heinemann SH (1995) Differential effects of high hydrostatic pressure on N- and C-type inactivation of cloned potassium channels. Pflügers Arch 426:R16

Murrell-Lagnado RD, Aldrich RW (1993) Interactions of amino terminal domains of *Shaker* K channels with a pore blocking site studied with synthetic peptides. J Gen Physiol 102:949–975

Nobile M, Olcese R, Toro L, Stefani E (1997) Fast inactivation of *Shaker* $K^+$ channels is highly temperature dependent. Exp Brain Res 114:138–142

Pahapill PA, Schlichter LC (1990) Modulation of potassium channels in human T-lymphocytes: effects of temperature. J Physiol 422:103–126

Rasmusson RL, Morales MJ, Castellino RC, Ying Z, Campell DL, Strauss HC (1995) C-type inactivation controls recovery in a fast inactivating cardiac $K^+$ channel (Kv1.4) expressed in *Xenopus* oocytes. J Physiol 489:709–721

Rodríguez BM, Bezanilla F (1996) Transitions near the open state in *Shaker* $K^+$-channel: Probing with temperature. Neuropharmacol 35:775–785

Schlief T, Schönherr R, Heinemann SH (1996) Modification of C-type inactivating *Shaker* potassium channels by chloramine-T. Pflügers Arch 431:483–493

Starkus JG, Schlief T, Rayner MD, Heinemann SH (1995). Unilateral exposure of *Shaker* B potassium channels to hyperosmolar solution. Biophys J 69:860–872

Stühmer W, Terlau H, Heinemann SH (1992) *Xenopus* oocytes for two electrode and patch clamp recording. In: Kettenmann H, Grantyn R (eds) Practical electro-physiological methods. Wiley-Liss, New York, pp 121–125